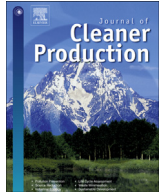




Contents lists available at ScienceDirect

Journal of Cleaner Production

journal homepage: www.elsevier.com/locate/jclepro

Optimal scheduling of electric vehicles and photovoltaic systems in residential complexes under real-time pricing mechanism

Sahar Seyyede Barhagh^{a, *}, Mehdi Abapour^a, Behnam Mohammadi-Ivatloo^{a, b}

^a Faculty of Electrical and Computer Engineering, University of Tabriz, Tabriz, Iran

^b Institute of Research and Development, Duy Tan University, Da Nang 550000, Vietnam

ARTICLE INFO

Article history:

Received 4 October 2018

Received in revised form

19 October 2019

Accepted 24 October 2019

Available online xxx

Handling Editor: Prof. Jiri Jaromir Klemes

Keywords:

Residential complex (RC)

Economic performance

Photovoltaic (PV) system

Electric vehicle (EV)

Real-time pricing (RTP) of demand response program (DRP)

ABSTRACT

Residential complexes (RCs) consisting of photovoltaic (PV) systems, wind turbines and electric vehicles (EVs), have been rapidly extended in energy systems in recent years. Optimal scheduling of local generation units can lead to economic improvement in RCs. In this regard, optimization of the performance of RCs appears to be necessary. Operators of RC energy systems equipped with local generation units can benefit from demand response programs (DRPs) to reduce their operating costs while satisfying energy demands. Within these programs, energy consumers are motivated to change their consumption in a way that economic targets are satisfied. In this paper, optimal operation of a grid-connected EV/PV RC energy system is studied under real-time pricing of a DRP. The studied RC energy system is equipped with PV units and EVs that can support RCs in supplying energy demands and providing economic benefits. The incorporated PV unit is modeled considering solar irradiance parameters and ambient temperature, which can lead to accurate simulation results. Moreover, the proposed model for EVs can enhance the efficient operation of RCs through optimal charge and discharge processes. Further, the optimal operation of energy systems integrated into RCs is modeled as mixed-integer linear programming (MILP). Additionally, a general algebraic modeling system (GAMS) is used to carry out simulations in different scenarios and the results are presented for comparison. For the studied test case, the total expected cost of RCs is reduced by 37.31%, which represents the influential impact of demand response on the optimal scheduling of DG units.

© 2019 Elsevier Ltd. All rights reserved.

1. Introduction

Nowadays, due to the crises induced by fossil fuel over-consumption, renewable energy sources such as wind turbines (Fathabadi, 2017; Mirzaei et al., 2019; Shezan et al., 2016) and photovoltaic (PV) systems (Bukar and Tan, 2019; Majidi et al., 2017; Shezan et al., 2016) have been extensively used in power systems. These sources generate clean and inexpensive energy to satisfy energy demands. However, the intermittent generation of these sources can cause many problems for operators of energy systems. In order to handle these issues, electric vehicles (EVs) (Aliasghari et al., 2018; Fathabadi, 2018; Li et al., 2018; Lu et al., 2018; Sedighizadeh et al., 2018) can be integrated with other energy sources in power systems.

In this section, a summary of studies about the operation of

residential microgrid energy systems under incorporation of distributed generation (DG) units in various fields is presented.

Renewable sources have been among the most suitable options for energy sources in microgrids. Different types of these sources have been integrated into microgrids to satisfy different objectives. For instance, the energy management problem was studied in microgrids consisting of solar and wind units, boilers, micro-turbines, CHP and energy storage systems under different loads (Tabar et al., 2017). Moreover, a residential microgrid containing a mini-size wind turbine and PV panels was managed using a novel strategy to improve the grid power profile and reduce power peaks (Pascual et al., 2015). In another investigation (Sreedharan et al., 2016), different strategies were used to minimize the monthly energy bill of the University of California-San Diego by integrating renewable energy sources. Implementing the genetic algorithm, unit commitment problem and the economic dispatch problem of renewable units in microgrids were evaluated (Nemati et al., 2018). Moreover, the optimum energy management of microgrids was studied to reduce the total cost of buying power from different

* Corresponding author.

E-mail address: sbarhagh95@ms.tabrizu.ac.ir (S. Seyyede Barhagh).

Nomenclature		Parameters	
Indices		η_t^{chev}	Rate of charge of EV
t	Time period index	η_t^{dchev}	Rate of discharge of EV
s	Scenario index	λ_t^{imp}	Price of imported electric power from the upstream grid
Variables		λ_t^{exp}	Price of exported electric power to the upstream grid
$cost$	Total operation cost of RC	θ_β	The incidence angle of solar radiation on a tilted surface
$I_{d,s}$	Direct normal irradiance	β	A tilted angle
$I_{dif,s}$	Diffuse horizontal irradiance	ρ	Surrounding reflection
$I_{g,s}$	Global horizontal irradiance	Π_s	Scenario probability
$p_{load,NC}^{DRP,t,s}$	Non-critical load under RTP	α	Temperature coefficient of PV systems
$p_{load,C}^{t,s}$	Critical load	E	Demand-price elasticity coefficient
$p_{load,NC}^{t,s}$	Non-critical load	M_t	Availability of EV
$p_{t,s}^{imp}$	Imported power from the upstream grid	n_s^{PV}	PV panel numbers in series
$p_{t,s}^{exp}$	Exported power to the upstream grid	n_p^{PV}	PV panel numbers in parallel
$p_{t,s}^{chev}$	Charge power of EV	$NOCT$	Nominal temperature of the operating cell
$p_{t,s}^{dchev}$	Discharge power of EV	$p_{t,s}^{imp,min}$	Minimum imported power from the upstream grid
$p_{t,s}^{pv}$	Output power of PV systems	$p_{t,s}^{imp,max}$	Maximum imported power from the upstream grid
$SOC_{t,s}$	State of charge of EV	$p_{t,s}^{exp,min}$	Minimum exported power to the upstream grid
$SOC_{t,s}^{Arrive}$	State of charge of EV at arrival time per scenario	$p_{t,s}^{exp,max}$	Maximum exported power to the upstream grid
$SOC_{t,s}^{Dep}$	State of charge of EV at departure time	$p_{t,s}^{chev,max}$	Maximum charge power of EV
$T_{t,s}^a$	Ambient temperature	$p_{t,s}^{dchev,max}$	Maximum discharge power of EV
$T_{t,s}^c$	Temperature of cells	$p_{t,s}^{pv,max}$	The PV output at the maximum power point and the standard test condition
Binary Variables		$p_{t,s}^{pv,stc}$	Maximum power of the PV converter
$B_{t,s}^{ch}$	A binary variable of EV's charging condition	$p_{t,s}^{pv,max}$	Real-time power price
$B_{t,s}^{dch}$	A binary variable of EV's discharging condition	$RT_{price,t}$	Minimum state of charge of EV
$I_{t,s}^{imp}$	A binary variable for power import	SOC_{min}	Maximum state of charge of EV
$I_{t,s}^{exp}$	A binary variable for power export	SOC_{max}	Maximum state of charge of EV at arrival time
		$SOC_{t,s}^{Arrive}$	Maximum state of charge of EV at departure time
		$SOC_{t,s}^{Dep}$	Desired state of charge of EV at departure time
		$SOC_{t,s}^{desired}$	Scenario number
		SN	Scheduling horizon
		T	

sources like as PV units, wind turbines, hydro-electric units, thermal units and gas-fired power generation systems (Abedini et al., 2016). In another work (Numbi and Malinga, 2017), the cost-effective performance of a PV-based residential microgrid energy system was examined under feed-in tariff, in which the payback index was employed to assess the economic operation of the studied system.

Renewable-based microgrids can be stable enough to supply energy consumers in islanded/isolated operation modes. In ref (Rokni et al., 2018), a distributed energy management methodology was implemented based-on alternating direction method of multipliers to optimize the performance of grid-connected/islanded PV-based microgrids under power flow limitations. In order to control the operation of an isolated microgrid that includes renewable energy sources, a robust technique was provided to avoid frequency instabilities in probable contingencies (Kerdphol et al., 2018). Microgrids may include different types of distributed energy sources (DERs) including renewable and non-renewable. In order to share power among coupled DERs in an autonomous islanded microgrid under unbalanced loads, a robust control methodology was employed (Gholami et al., 2018). Moreover, the optimal design of hybrid electric power generation systems including renewable units such as PVs were obtained for isolated zones using meta-heuristic optimization techniques such as particle swarm optimization (Galindo Noguera et al., 2018).

Integrating renewable sources can result in hybrid energy systems for various applications in power systems, especially in microgrids. The optimal planning and design of hybrid renewable

energy systems for microgrid applications was obtained using the distributed energy resources customer adoption model in (Jung and Villaran, 2017). Authors in ref (Fathabadi, 2018b), presented a novel model to replace internal combustion engine of vehicles with renewable units such as wind turbines and PV systems. Moreover, in (Zehir et al., 2017), the operation analysis of secondary distribution networks comprising renewable-based microgrids was focused on to solve distribution network related problems such as voltage instabilities, power losses, etc.

Optimal sizing and siting of renewable units in microgrids were also considered in some researches. In the research presented in (Pesaran H.A et al., 2017), optimum placement problems of DG units including renewable sources were reviewed in terms of different parameters such as type of problem, utilized methods, etc. In ref (Hong et al., 2017), renewable energy generation sources were optimally sized in a community microgrid using a novel method based on the Markov model and by incorporating the interior-point algorithm.

Demand side management programs were implemented in research papers to improve the performance of microgrids. By implementing two demand response programs (DRPs) based on time-of-use and real-time pricing (RTP) in (Nikmehr et al., 2017), the optimal day-ahead scheduling of microgrids consisting of different types of renewable energy sources was studied to minimize total operation cost with the use of particle swarm optimization (PSO). In (Aghajani et al., 2017), demand response packages were proposed as options for controlling renewable uncertainties. Moreover the multi-follower bi-level programming was used to

minimize the energy cost of the distribution network operator under the assumption of multi-microgrids and DRPs (Jalali et al., 2017). Furthermore, a multi-objective energy management system was provided, in which the microgrid performance was optimized in the presence of uncertainty of renewable units and demand response providers (Aghajani et al., 2015). Demand response providers cover the uncertainties of wind units and PV systems. In this regard, the optimum component size of microgrids was obtained using a DRP to balance the generation and consumption of energy and peak load and minimize their cost (Amrollahi and Bathaee, 2017). Similar problems have also been studied along with EV scheduling (Zifa Liu et al., 2018; SoltaniNejad Farsangi et al., 2018).

As one of the novel technologies being rapidly expanded in energy systems, especially in microgrids, EVs have been incorporated to improve the operation of microgrids by providing various services. The impact of integrating different types of EVs with various characteristics and renewable units into the power systems was investigated (Fathabadi, 2015). In order to handle the optimal operation of microgrids in the presence of plug-in hybrid electric vehicles (PHEVs), robust optimization was employed to minimize the operation cost of microgrids while taking possible risks into account (Bahramara and Golpira, 2018). In (Kamankesh et al., 2016), the implementation of a new robust and symbiotic organism search (SOS) algorithm for optimal energy management of microgrids containing PHEVs, storage devices and renewable energy sources was evaluated, in which the overall system covering cost of local generation units as well as cost of interaction between the upstream network and the microgrid was minimized. By implementing a new optimization algorithm based on the bat algorithm, optimal scheduling of electric power units was studied in renewable-based local distribution systems including PHEVs, in which the total network cost including cost of energy not supplied, reliability cost and cost of power supply for loads and PHEVs was minimized (Tabatabaee et al., 2017). By solving the non-linear optimization, an optimal day-ahead operation plan of microgrids was obtained to decrease the operation cost of microgrids under the optimum integration of EVs and by using the vehicle to grid (V2G) technology (Aluisio et al., 2017). Similarly, the V2G technology was employed to improve the operation of microgrids in unbalanced and isolated modes (Rodrigues et al., 2018), satisfy economic-environmental expectations and provide market opportunities with considering risks (Salehi and Gazijahani, 2018). The placement and sizing of V2G technologies in a microgrid were studied in (Mortaz et al., 2019).

Locations, in which energy systems such as charging stations are installed, play a key role in the operation of installed generation units. To analyze a location from different viewpoints, various factors should be taken into account and sufficient data from end-users should be collected, which can be achieved through innovative data collection technologies (Forati et al., 2015). In this regard, fast-charging stations were optimally located to maximize long-distance trip completion in the United States (He et al., 2019). It should be noted that with technology progress, wireless charging technologies have been innovated for EVs in recent years, which was summarized in (Machura and Li, 2019). With the aim of charging EVs by renewable energy sources and enhancing export capacity, the potential of smart charging of EVs was analyzed in (Pearre and Swan, 2016). In another investigation (Baccino et al., 2015), EVs were optimally scheduled in distribution networks, in which a novel optimization framework consisting of two stages was developed to take power flow constraints into account while optimizing the recharge power of EVs. To this end, first, power flow limitations were evaluated and, the optimum recharge power was obtained for EVs.

Penetration of EVs and control of their charge and discharge patterns in power systems could be challenged with different issues such as random arrival times. Optimum charge patterns were obtained for EVs through global and local scheduling schemes in ref (He et al., 2012). In doing so, a global scheduling scheme was developed to minimize the total cost considering the pre-known EV arrival. Moreover, a local scheduling scheme was developed to minimize the total cost in the current ongoing EV set in the local group. The results revealed that the local scheduling scheme led to closer optimization results. Similarly in ref (Sortomme and El-Sharkawi, 2012), a unidirectional vehicle to grid technology was employed to provide energy and ancillary services to an electricity network. According to the model proposed in their study, consumers and utilities can have the most optimal performance by benefiting from the provided options. In another research (Wu et al., 2019), a data-driven non-parametric joint chance-constrained optimization model was developed for the optimal economic dispatch of PV-based energy system, in which the uncertainty of power generated by a PV system was taken into account through the proposed model.

In this paper, a mathematical-based optimization framework is presented for energy management of a residential complex (RC) in South Africa, which includes a specific energy consumption pattern. The mentioned RC is a grid-connected energy system, in which renewable generation units such as PV systems as well as storage technologies such as EVs are integrated in order to enhance its performance from various viewpoints. PV systems can generate clean and inexpensive power to be used for either load supply or export process. The accurate modeling of PV generation is necessary to have real particle simulation results. Thus, a precise mathematical-based model is proposed to formulate the output power of PV systems. EVs can manage energy consumption within RC by handling the intermittent generation of PV systems through optimal charge and discharge processes. In fact, EVs can have bidirectional power exchange (charge/discharge) with the RC, and charge/discharge processes can help the RC optimize the energy consumption and control the intermittent generation of PV systems. The discharged power by EVs can be used to supply demand in peak-time periods, which can mitigate the negative economic impact of power imported from the upstream network in the mentioned periods. Similar to PV systems, a mathematical-based model is proposed to model the operation of EVs. In order to assess the performance of the RC toward DRPs, an RTP mechanism is proposed and the RC performance is evaluated from different economic viewpoints. It is worth mentioning that in order to optimize the energy system operation, different valuable methodologies have been previously introduced, one of which has been the chance constraint optimization method. This method is mostly used to solve optimization problems with considering probabilistic conditions (Zhaoxi Liu et al., 2018). At first, different scenarios with various probabilities are generated for uncertain parameters and, then according to this method, the probability of satisfying a specific constraint is ensured (Odetayo et al., 2018). The main focus of the proposed mathematical-based model is to optimally integrate renewable energy sources such as PV units as well as storage facilities such as EVs into RC systems that might include energy demands with different patterns. Moreover, the proposed model seeks to assess the impact of DRPs such as RTP on the economic performance of RCs in countries like South Africa. Therefore, contributions of the conducted study can be expressed as follows:

- The optimal operation of a renewable-based RC considering the real data of the city of Durba in South Africa;
- The utilization of EVs to handle the intermittent generation of PV systems and gain economic benefit;

- The implementation of RTP to improve the RC performance by reducing total operation cost;
- The proposal of a comprehensive optimization framework based on MILP for optimal energy management and uncertainty management in a grid-connected RC with local energy units.

Other parts of the conducted paper are classified as follows: Mathematical formulations are presented in Section 2. Simulations and corresponding results are presented in Section 3. Finally, conclusions are presented in Section 4.

2. Problem formulation

The proposed optimization model is mathematically formulated in this section for the economic performance of a grid-connected RC containing PV system and EV with RTP.

2.1. Objective function

As the objective function, the total cost of the RC including the cost of power imported from the RC minus the revenue obtained from power exported to the upstream grid should be minimized as in Eq. (1).

$$\text{Min } \text{obj} = \text{cost} = \left(\sum_s^{SN} \Pi_s \times \sum_t^T (P_{t,s}^{\text{imp}} \times \lambda_t^{\text{imp}} - P_{t,s}^{\text{exp}} \times \lambda_t^{\text{exp}}) \right) \times TP \quad (1)$$

where *obj* is the objective function, *cost* is the total operation cost of RC, *SN* is the number of scenarios, *s* is the scenario index, *T* is the scheduling horizon, *t* is the time period, $P_{t,s}^{\text{imp}}$ is the imported power from the upstream grid, λ_t^{imp} is the price of power imported from the upstream grid, $P_{t,s}^{\text{exp}}$ is power exported to the upstream grid, λ_t^{exp} is the price of power exported to the upstream grid and *TP* is the number of scheduling days.

2.2. Energy balance constraint

The required power for critical and non-critical loads is received from the output power of the PV system, the upstream grid and the discharge power of the EV. The mentioned explanations are mathematically modeled in Eq. (2).

$$p_{t,s}^{\text{load,C}} + p_{t,s}^{\text{load,Nc}} = P_{t,s}^{\text{pv}} + P_{t,s}^{\text{imp}} - P_{t,s}^{\text{exp}} + P_{t,s}^{\text{dchev}} - P_{t,s}^{\text{chev}} \quad (2)$$

where $p_{t,s}^{\text{load,C}}$ is the critical load, $p_{t,s}^{\text{load,Nc}}$ is the non-critical load, $P_{t,s}^{\text{chev}}$ is the charge power of the EV, $P_{t,s}^{\text{pv}}$ is the output power of the PV system and $P_{t,s}^{\text{dchev}}$ is the discharge power of the EV.

2.3. Distributed generation (DG) unit limitations

In this section, the limitations of DG units and the EV are presented through Eqs. (3)–(13).

2.3.1. Photovoltaic (PV) system

Renewable units such as PV systems can play positive roles in the optimal operation of energy systems. Power generated by these systems is usually intermittent. Therefore, accurate modeling of these units is necessary for accurate simulation results. The proposed model for the PV system in this paper is a comprehensive mathematical-based model taken from (Numbi and Malinga, 2017), according to which the output of the PV system is proportional to solar irradiance, cell temperature, number of PV panels in series

and parallel and other relevant factors. The proposed model is expressed in Eqs. (3)–(5) (Numbi and Malinga, 2017).

$$P_{t,s}^{\text{pv}} = P_{\text{stc}}^{\text{pv}} \times n_{\text{se}}^{\text{pv}} \times n_{\text{pa}}^{\text{pv}} \times I_{d,s} \times \cos \theta_{\beta} + I_{\text{dif},s} \times \frac{(1 + \cos \beta)}{2} + \rho \times I_{g,s} \times \frac{1 - \cos \theta_{\beta}}{1000} \times (1 - \alpha \times (T_{t,s}^{\text{c}} - 25)) \quad (3)$$

where $P_{\text{stc}}^{\text{pv}}$ is the PV output at the maximum power point and the standard test condition, $n_{\text{se}}^{\text{pv}}$ is the number of PV panels in series, $n_{\text{pa}}^{\text{pv}}$ is the number of PV panels in parallel, $I_{d,s}$ is the direct normal irradiance, θ_{β} is the incidence angle of solar radiation on a tilted surface, $I_{\text{dif},s}$ is the diffuse horizontal irradiance, β is the tilted angle, ρ is the surrounding reflection, $I_{g,s}$ is the global horizontal irradiance, α is the temperature coefficient of the PV system and $T_{t,s}^{\text{c}}$ is the temperature of cells.

The temperature of cells mentioned above is proportional to the ambient temperature, which is expressed in Eq. (4).

$$T_{t,s}^{\text{c}} = T_{t,s}^{\text{a}} + I_{d,s} \times \cos \theta_{\beta} + I_{\text{dif},s} \times \frac{(1 + \cos \beta)}{2} + \rho \times I_{g,s} \times \frac{1 - \cos \theta_{\beta}}{2 \times 800} \times (NOCT - 20) \quad (4)$$

where $T_{t,s}^{\text{a}}$ is the ambient temperature and *NOCT* is the nominal temperature of the operating cell.

The output power of the PV system should be within the legal nominal range as follows:

$$P_{t,s}^{\text{pv}} \leq P_{t,\text{max}}^{\text{mppt}} \quad (5)$$

where $P_{t,\text{max}}^{\text{mppt}}$ is the maximum power of the converter.

2.3.2. Electric vehicle model

The integrated EV is modeled through Eqs. (6)–(13) (Jannati and Nazarpour, 2017). EVs can optimally charge and discharge power to optimize energy consumption in RCs. However, there are some limitations such as availability of EVs, charge and discharge rates and others that should be taken into account in modeling such energy units. The total charge power of the EV with regard to its availability should be less than the rated charge value, which is expressed in Eq. (6). Moreover, the discharge power of the EV

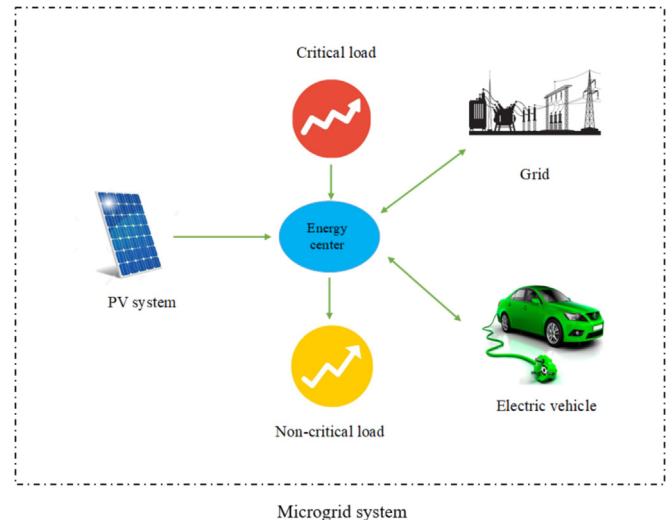


Fig. 1. Studied PV-EV-based RC

Table 1

The scenario's probability.

Scenario	Probability	Scenario	Probability
1	0.04	11	0.04
2	0.06	12	0.05
3	0.02	13	0.07
4	0.09	14	0.03
5	0.05	15	0.04
6	0.06	16	0.05
7	0.07	17	0.06
8	0.09	18	0.01
9	0.08	19	0.03
10	0.05	20	0.01

Table 2

The SOC value at the arrival time of the EV.

Scenario	$SOC_{t,s}^{Arrive}$ (kWh)	Scenario	$SOC_{t,s}^{Arrive}$ (kWh)
1	0.6537	11	0.5397
2	0.6789	12	0.7134
3	0.5316	13	0.7031
4	0.6817	14	0.5978
5	0.6203	15	0.6506
6	0.5223	16	0.5357
7	0.5648	17	0.5882
8	0.6071	18	0.6826
9	0.7033	19	0.6488
10	0.7086	20	0.7047

within the available period is limited to be less than the nominal discharge rate, which is expressed in Eq. (7). Finally, when the EV is available, charge and discharge processes should not occur at the same time, which is expressed in Eq. (8).

$$P_{t,s}^{chev} \leq P_{max}^{chev} \times B_{t,s}^{ch} \times M_t \quad (6)$$

where $P_{t,s}^{chev}$ is the charging power of the EV, P_{max}^{chev} is the maximum charge power of the EV, $B_{t,s}^{ch}$ is the binary variable of the EV charging condition and M_t is the availability of the EV.

Table 3

The critical load value per scenario.

Time	$p_{t,s}^{load,C}$ (kW)																			
	1	2	3	4	5	6	7	8	9	10	11	12	13	14	15	16	17	18	19	20
1	0.0	0.0	0.0	0.0	0.0	0.0	0.0	0.0	0.0	0.0	0.0	0.0	0.0	0.0	0.0	0.0	0.0	0.0	0.0	0.0
2	0.2	0.3	0.3	0.3	0.3	0.2	0.2	0.3	0.2	0.3	0.3	0.3	0.3	0.3	0.3	0.2	0.2	0.3	0.3	0.2
3	0.3	0.2	0.3	0.3	0.2	0.2	0.2	0.2	0.2	0.3	0.2	0.3	0.3	0.3	0.2	0.3	0.2	0.3	0.2	0.2
4	0.2	0.3	0.2	0.2	0.3	0.2	0.3	0.2	0.3	0.2	0.3	0.3	0.3	0.3	0.2	0.3	0.3	0.3	0.2	0.2
5	0.0	0.0	0.0	0.0	0.0	0.0	0.0	0.0	0.0	0.0	0.0	0.0	0.0	0.0	0.0	0.0	0.0	0.0	0.0	0.0
6	0.2	0.2	0.2	0.3	0.3	0.2	0.2	0.3	0.3	0.3	0.3	0.3	0.2	0.3	0.2	0.2	0.3	0.3	0.2	0.3
7	0.3	0.3	0.3	0.3	0.3	0.2	0.3	0.3	0.2	0.3	0.2	0.3	0.2	0.2	0.2	0.2	0.2	0.3	0.3	0.3
8	0.2	0.3	0.3	0.3	0.2	0.2	0.3	0.3	0.2	0.2	0.3	0.2	0.3	0.2	0.2	0.3	0.3	0.3	0.2	0.2
9	0.0	0.0	0.0	0.0	0.0	0.0	0.0	0.0	0.0	0.0	0.0	0.0	0.0	0.0	0.0	0.0	0.0	0.0	0.0	0.0
10	0.3	0.3	0.2	0.3	0.2	0.2	0.3	0.3	0.3	0.3	0.2	0.3	0.2	0.3	0.3	0.3	0.2	0.3	0.3	0.2
11	0.3	0.3	0.3	0.2	0.3	0.2	0.3	0.2	0.2	0.3	0.3	0.2	0.3	0.3	0.3	0.2	0.2	0.3	0.2	0.2
12	0.3	0.3	0.3	0.3	0.2	0.2	0.2	0.2	0.3	0.3	0.2	0.3	0.2	0.3	0.2	0.3	0.2	0.3	0.3	0.2
13	0.0	0.0	0.0	0.0	0.0	0.0	0.0	0.0	0.0	0.0	0.0	0.0	0.0	0.0	0.0	0.0	0.0	0.0	0.0	0.0
14	0.2	0.2	0.2	0.2	0.2	0.2	0.3	0.2	0.3	0.2	0.2	0.2	0.3	0.3	0.3	0.3	0.3	0.2	0.2	0.2
15	0.5	0.5	0.5	0.6	0.5	0.4	0.6	0.5	0.5	0.5	0.6	0.5	0.5	0.5	0.5	0.5	0.5	0.5	0.5	0.5
16	0.5	0.4	0.5	0.5	0.5	0.5	0.5	0.4	0.4	0.5	0.5	0.6	0.6	0.5	0.5	0.6	0.5	0.6	0.6	0.5
17	0.3	0.3	0.2	0.2	0.3	0.3	0.2	0.3	0.3	0.3	0.2	0.3	0.3	0.3	0.2	0.3	0.2	0.2	0.2	0.3
18	0.6	0.5	0.5	0.5	0.5	0.6	0.6	0.6	0.5	0.5	0.5	0.5	0.6	0.6	0.5	0.5	0.4	0.6	0.5	0.5
19	1.9	1.8	1.9	1.6	1.7	1.7	1.5	1.6	1.6	1.8	1.6	1.9	1.8	1.6	1.7	1.7	1.8	1.7	1.7	1.6
20	1.6	1.8	1.9	1.8	1.3	1.7	1.6	1.6	1.5	1.8	1.6	1.5	1.6	1.6	1.7	1.7	1.6	1.6	1.7	1.7
21	2.1	1.9	1.8	2.0	1.6	1.5	1.6	1.6	1.7	1.7	1.4	1.8	1.6	1.6	1.9	2.0	2.2	1.8	2.3	1.8
22	2.0	1.9	2.0	2.0	1.7	2.2	1.7	2.0	2.2	1.9	2.1	2.2	2.2	2.3	1.8	1.9	2.3	2.0	2.0	2.1
23	2.0	1.8	1.6	1.8	1.8	2.1	1.9	1.9	1.9	1.7	1.8	1.8	1.6	1.8	1.9	1.8	2.0	1.9	1.7	1.8
24	0.2	0.3	0.3	0.2	0.3	0.3	0.3	0.3	0.2	0.2	0.3	0.2	0.2	0.2	0.3	0.2	0.3	0.2	0.3	0.3

$$P_{t,s}^{dchev} \leq P_{max}^{dchev} \times B_{t,s}^{dch} \times M_t \quad (7)$$

where $P_{t,s}^{dchev}$ is the discharge power of the EV, P_{max}^{dchev} is the maximum discharge power of the EV and $B_{t,s}^{dch}$ is the binary variable of the EV discharging condition.

$$B_{t,s}^{ch} + B_{t,s}^{dch} \leq M_t \quad (8)$$

The state of charge (SOC) of the EV at present hour depends on SOC in previous hour and charge and discharge processes. The SOC of the EV is mathematically expressed in Eq. (9).

$$SOC_{t,s} = SOC_{t-1,s} + P_{t,s}^{chev} \times \eta_t^{chev} - \frac{P_{t,s}^{dchev}}{\eta_t^{dchev}} \quad (9)$$

where $SOC_{t,s}$ is the SOC of the EV, η_t^{chev} is the rate of charge of the EV and η_t^{dchev} is the rate of discharge of the EV.

The SOC of the EV is limited by Eq. (10).

$$SOC_{min} \leq SOC_{t,s} \leq SOC_{max} \quad (10)$$

where SOC_{min} and SOC_{max} are the minimum and maximum SOC of the EV, respectively.

The limitations related to the SOC of the EV at arrival and departure time are expressed in Eqs.(11)–(13). It is worth mentioning that in order to consider different driving patterns, the scenario-based methodology is utilized to generate scenarios in order to model the stochastic nature of the SOC value at the arrival time of the EV.

$$SOC_{t,s}^{Arrive} \leq SOC_{Max}^{Arrive} \quad (11)$$

where $SOC_{t,s}^{Arrive}$ is the SOC of the EV at arrival time and SOC_{Max}^{Arrive} is the maximum SOC of the EV at arrival time.

$$SOC_{t,s}^{Dep} \leq SOC_{desired}^{Dep} \quad (12)$$

Table 4

The non-critical load value per scenario.

Time	$p_{t,s}^{load,nc}$ (kW)																			
	1	2	3	4	5	6	7	8	9	10	11	12	14	14	15	16	17	18	19	20
1	0.0	0.0	0.0	0.0	0.0	0.0	0.0	0.0	0.0	0.0	0.0	0.0	0.0	0.0	0.0	0.0	0.0	0.0	0.0	0.0
2	0.0	0.0	0.0	0.0	0.0	0.0	0.0	0.0	0.0	0.0	0.0	0.0	0.0	0.0	0.0	0.0	0.0	0.0	0.0	0.0
3	0.0	0.0	0.0	0.0	0.0	0.0	0.0	0.0	0.0	0.0	0.0	0.0	0.0	0.0	0.0	0.0	0.0	0.0	0.0	0.0
4	0.0	0.0	0.0	0.0	0.0	0.0	0.0	0.0	0.0	0.0	0.0	0.0	0.0	0.0	0.0	0.0	0.0	0.0	0.0	0.0
5	2.0	1.9	2.2	2.4	1.6	2.0	1.7	2.2	2.5	1.7	2.3	1.6	2.1	2.2	2.0	2.2	2.3	2.1	1.8	1.8
6	1.8	1.7	1.8	2.1	2.3	1.9	2.0	2.4	2.3	2.1	2.5	2.1	1.9	2.1	1.9	1.9	2.1	2.0	2.0	2.1
7	0.0	0.0	0.0	0.0	0.0	0.0	0.0	0.0	0.0	0.0	0.0	0.0	0.0	0.0	0.0	0.0	0.0	0.0	0.0	0.0
8	0.0	0.0	0.0	0.0	0.0	0.0	0.0	0.0	0.0	0.0	0.0	0.0	0.0	0.0	0.0	0.0	0.0	0.0	0.0	0.0
9	0.0	0.0	0.0	0.0	0.0	0.0	0.0	0.0	0.0	0.0	0.0	0.0	0.0	0.0	0.0	0.0	0.0	0.0	0.0	0.0
10	0.0	0.0	0.0	0.0	0.0	0.0	0.0	0.0	0.0	0.0	0.0	0.0	0.0	0.0	0.0	0.0	0.0	0.0	0.0	0.0
11	0.0	0.0	0.0	0.0	0.0	0.0	0.0	0.0	0.0	0.0	0.0	0.0	0.0	0.0	0.0	0.0	0.0	0.0	0.0	0.0
12	0.0	0.0	0.0	0.0	0.0	0.0	0.0	0.0	0.0	0.0	0.0	0.0	0.0	0.0	0.0	0.0	0.0	0.0	0.0	0.0
13	0.0	0.0	0.0	0.0	0.0	0.0	0.0	0.0	0.0	0.0	0.0	0.0	0.0	0.0	0.0	0.0	0.0	0.0	0.0	0.0
14	0.0	0.0	0.0	0.0	0.0	0.0	0.0	0.0	0.0	0.0	0.0	0.0	0.0	0.0	0.0	0.0	0.0	0.0	0.0	0.0
15	0.0	0.0	0.0	0.0	0.0	0.0	0.0	0.0	0.0	0.0	0.0	0.0	0.0	0.0	0.0	0.0	0.0	0.0	0.0	0.0
16	0.0	0.0	0.0	0.0	0.0	0.0	0.0	0.0	0.0	0.0	0.0	0.0	0.0	0.0	0.0	0.0	0.0	0.0	0.0	0.0
17	0.0	0.0	0.0	0.0	0.0	0.0	0.0	0.0	0.0	0.0	0.0	0.0	0.0	0.0	0.0	0.0	0.0	0.0	0.0	0.0
18	0.0	0.0	0.0	0.0	0.0	0.0	0.0	0.0	0.0	0.0	0.0	0.0	0.0	0.0	0.0	0.0	0.0	0.0	0.0	0.0
19	4.1	3.9	4.0	3.4	3.8	3.8	3.2	3.5	3.4	3.8	3.4	4.1	3.9	3.5	3.6	3.8	3.9	3.7	3.7	3.4
20	2.0	2.1	2.2	2.1	1.6	2.1	2.0	2.0	1.8	2.2	1.9	1.9	1.9	1.9	2.0	2.0	1.9	1.9	2.0	2.1
21	0.5	0.5	0.4	0.5	0.4	0.4	0.4	0.4	0.4	0.4	0.3	0.4	0.4	0.4	0.4	0.5	0.4	0.5	0.4	0.4
22	0.4	0.4	0.4	0.4	0.4	0.5	0.4	0.4	0.5	0.4	0.4	0.5	0.5	0.5	0.4	0.4	0.5	0.4	0.4	0.4
23	0.0	0.0	0.0	0.0	0.0	0.0	0.0	0.0	0.0	0.0	0.0	0.0	0.0	0.0	0.0	0.0	0.0	0.0	0.0	0.0
24	0.0	0.0	0.0	0.0	0.0	0.0	0.0	0.0	0.0	0.0	0.0	0.0	0.0	0.0	0.0	0.0	0.0	0.0	0.0	0.0

$$SOC_{desired}^{Dep} = SOC_{max} \quad (13)$$

where $SOC_{t,s}^{Dep}$ is the SOC of the EV at departure time and $SOC_{desired}^{Dep}$ is the desired SOC of the EV at departure time.

2.3.3. Upstream grid

Power exported from the RC grid to the upstream grid and power imported from the upstream grid to the RC grid are limited by Eqs.(14) and (15). According to Eq. (14), total exported power cannot exceed the nominal power of the line connecting the RC to

the upstream grid. Moreover, as expressed in Eq. (15), total imported power should be within the nominal limitation of the mentioned line. Finally, Eq. (16) is used to limit the simultaneous import and export of power. Specifically, when power is exported, the binary variable $I_{t,s}^{exp}$ is equal to 1. Similarly, when power is imported, the binary variable $I_{t,s}^{imp}$ is equal to 1. Therefore, according to Eq. (16), import and export processes cannot occur simultaneously.

$$I_{t,s}^{exp} \times P_{min}^{exp} \leq P_{t,s}^{exp} \leq I_{t,s}^{exp} \times P_{max}^{exp} \quad (14)$$

where $I_{t,s}^{exp}$ is the binary variable for power export and, P_{max}^{exp} and

Table 5

Direct normal irradiance per scenario.

Time	$I_{d,s}$ (w/m ²)																			
	1	2	3	4	5	6	7	8	9	10	11	12	14	14	15	16	17	18	19	20
1	0	0	0	0	0	0	0	0	0	0	0	0	0	0	0	0	0	0	0	0
2	0	0	0	0	0	0	0	0	0	0	0	0	0	0	0	0	0	0	0	0
3	0	0	0	0	0	0	0	0	0	0	0	0	0	0	0	0	0	0	0	0
4	0	0	0	0	0	0	0	0	0	0	0	0	0	0	0	0	0	0	0	0
5	0	0	0	0	0	0	0	0	0	0	0	0	0	0	0	0	0	0	0	0
6	376	342	362	426	478	398	404	503	480	433	508	444	396	431	385	392	433	417	405	425
7	644	616	611	616	605	520	639	764	581	718	580	676	597	590	556	534	573	640	651	634
8	595	854	886	833	642	752	818	823	717	728	811	772	800	720	704	850	832	893	680	706
9	736	843	772	951	736	701	857	908	803	767	810	777	847	956	873	737	821	710	845	830
10	1160	985	902	1018	806	880	1037	1031	956	932	869	1043	801	961	939	993	882	966	993	864
11	943	1121	943	890	959	898	996	911	929	978	1110	890	1023	991	1088	759	897	970	877	862
12	983	961	952	970	776	895	920	866	984	1030	877	988	830	1022	830	952	899	1012	932	929
13	1039	896	919	1098	770	1110	849	971	951	973	898	960	1013	738	803	1113	967	863	908	823
14	857	854	874	820	878	807	1023	794	1049	890	761	877	971	989	924	958	1028	768	867	760
15	709	821	822	866	792	662	886	841	732	784	944	820	853	763	770	788	728	828	777	805
16	606	569	634	616	689	687	666	567	509	648	605	737	770	602	692	718	654	714	739	646
17	604	580	458	561	590	572	550	656	623	628	551	582	634	654	594	522	592	486	556	594
18	0	0	0	0	0	0	0	0	0	0	0	0	0	0	0	0	0	0	0	0
19	0	0	0	0	0	0	0	0	0	0	0	0	0	0	0	0	0	0	0	0
20	0	0	0	0	0	0	0	0	0	0	0	0	0	0	0	0	0	0	0	0
21	0	0	0	0	0	0	0	0	0	0	0	0	0	0	0	0	0	0	0	0
22	0	0	0	0	0	0	0	0	0	0	0	0	0	0	0	0	0	0	0	0
23	0	0	0	0	0	0	0	0	0	0	0	0	0	0	0	0	0	0	0	0
24	0	0	0	0	0	0	0	0	0	0	0	0	0	0	0	0	0	0	0	0

Table 6
Diffuse horizontal irradiance per scenario.

Time	$I_{dif,s}$ (w/m ²)																			
	1	2	3	4	5	6	7	8	9	10	11	12	14	14	15	16	17	18	19	20
1	0	0	0	0	0	0	0	0	0	0	0	0	0	0	0	0	0	0	0	0
2	0	0	0	0	0	0	0	0	0	0	0	0	0	0	0	0	0	0	0	0
3	0	0	0	0	0	0	0	0	0	0	0	0	0	0	0	0	0	0	0	0
4	0	0	0	0	0	0	0	0	0	0	0	0	0	0	0	0	0	0	0	0
5	0	0	0	0	0	0	0	0	0	0	0	0	0	0	0	0	0	0	0	0
6	125	114	121	142	159	133	135	168	160	144	169	148	132	144	128	131	144	139	135	142
7	331	317	314	317	311	267	328	393	299	369	298	348	307	304	286	275	295	329	335	326
8	132	190	197	185	143	167	182	183	159	162	180	171	178	160	156	189	185	198	151	157
9	120	138	126	155	120	115	140	148	131	125	132	127	138	156	143	120	134	116	138	136
10	177	150	138	155	123	134	158	157	146	142	132	159	122	147	143	151	134	147	152	132
11	140	166	140	132	142	133	148	135	138	145	165	132	152	147	161	112	133	144	130	128
12	146	142	141	144	115	133	136	128	146	153	130	147	123	152	123	141	133	150	138	138
13	154	133	136	163	114	165	126	144	141	144	133	142	150	109	119	165	143	128	135	122
14	130	129	132	124	133	122	155	120	158	135	115	132	147	149	140	145	155	116	131	115
15	142	164	164	173	158	132	177	168	146	157	189	164	170	152	154	157	146	165	155	161
16	149	140	156	152	170	169	164	140	125	159	149	181	190	148	170	177	161	176	182	159
17	148	142	112	137	144	140	135	160	152	153	135	142	155	160	145	128	145	119	136	145
18	0	0	0	0	0	0	0	0	0	0	0	0	0	0	0	0	0	0	0	0
19	0	0	0	0	0	0	0	0	0	0	0	0	0	0	0	0	0	0	0	0
20	0	0	0	0	0	0	0	0	0	0	0	0	0	0	0	0	0	0	0	0
21	0	0	0	0	0	0	0	0	0	0	0	0	0	0	0	0	0	0	0	0
22	0	0	0	0	0	0	0	0	0	0	0	0	0	0	0	0	0	0	0	0
23	0	0	0	0	0	0	0	0	0	0	0	0	0	0	0	0	0	0	0	0
24	0	0	0	0	0	0	0	0	0	0	0	0	0	0	0	0	0	0	0	0

P_{min}^{exp} are, respectively, the maximum and minimum power exported to the upstream grid.

$$I_{t,s}^{imp} \times P_{min}^{imp} \leq P_{t,s}^{imp} \leq I_{t,s}^{imp} \times P_{max}^{imp} \quad (15)$$

where $I_{t,s}^{imp}$ is the binary variable for power import and, P_{min}^{imp} and P_{max}^{imp} are, respectively, the maximum and minimum power imported from the upstream grid.

$$I_{t,s}^{exp} + I_{t,s}^{imp} \leq 1 \quad (16)$$

2.3.4. Real-time pricing (RTP) mechanism

In some hours within a day, due to peak power consumption, the price of electricity increases and, therefore, total energy consumption cost within the mentioned periods increases proportionally. One option to handle energy consumption in such periods is DRPs. DRPs can help consumers manage their consumption efficiently to reduce their payments. In this paper, the RTP of DRP is used, which enables consumers to revise their consumption pattern according to the rates of energy determined previously. RTP is formulated in Eq. (17) (Numbi and Malinga, 2017).

Table 7
Global horizontal irradiance per scenario.

Time	$I_{g,s}$ (w/m ²)																			
	1	2	3	4	5	6	7	8	9	10	11	12	14	14	15	16	17	18	19	20
1	0	0	0	0	0	0	0	0	0	0	0	0	0	0	0	0	0	0	0	0
2	0	0	0	0	0	0	0	0	0	0	0	0	0	0	0	0	0	0	0	0
3	0	0	0	0	0	0	0	0	0	0	0	0	0	0	0	0	0	0	0	0
4	0	0	0	0	0	0	0	0	0	0	0	0	0	0	0	0	0	0	0	0
5	0	0	0	0	0	0	0	0	0	0	0	0	0	0	0	0	0	0	0	0
6	70	64	67	79	89	74	75	94	89	80	94	83	74	80	72	73	81	78	75	79
7	492	471	467	471	462	397	488	584	444	549	443	517	456	451	425	408	438	489	497	484
8	501	720	747	702	541	634	689	694	604	614	683	650	675	607	593	716	702	753	573	595
9	704	806	738	909	704	670	819	868	768	733	774	743	810	914	834	705	785	678	808	794
10	1282	1088	996	1125	891	972	1146	1139	1056	1030	960	1152	885	1062	1038	1097	974	1067	1098	954
11	1052	1250	1051	993	1070	1001	1111	1016	1037	1091	1238	992	1141	1105	1214	846	1000	1082	978	962
12	1137	1111	1102	1122	897	1035	1064	1001	1138	1191	1015	1143	960	1183	960	1101	1040	1170	1078	1074
13	1116	962	987	1179	828	1193	912	1043	1022	1045	964	1031	1088	793	862	1196	1039	927	976	884
14	835	832	851	799	855	786	996	773	1021	867	741	854	946	963	900	933	1001	748	844	740
15	633	733	733	773	707	591	791	751	653	700	842	732	761	681	687	703	650	739	693	718
16	503	472	527	511	572	571	553	471	423	538	502	612	640	500	575	597	543	593	614	537
17	245	235	186	228	239	232	223	266	253	255	223	236	257	265	241	212	240	197	225	241
18	0	0	0	0	0	0	0	0	0	0	0	0	0	0	0	0	0	0	0	0
19	0	0	0	0	0	0	0	0	0	0	0	0	0	0	0	0	0	0	0	0
20	0	0	0	0	0	0	0	0	0	0	0	0	0	0	0	0	0	0	0	0
21	0	0	0	0	0	0	0	0	0	0	0	0	0	0	0	0	0	0	0	0
22	0	0	0	0	0	0	0	0	0	0	0	0	0	0	0	0	0	0	0	0
23	0	0	0	0	0	0	0	0	0	0	0	0	0	0	0	0	0	0	0	0
24	0	0	0	0	0	0	0	0	0	0	0	0	0	0	0	0	0	0	0	0

Table 8
Ambient temperature per scenario.

Time	$T_{t,s}^a$ ($^{\circ}\text{C}$)																			
	1	2	3	4	5	6	7	8	9	10	11	12	14	14	15	16	17	18	19	20
1	19.9	22.6	21.5	22.8	21.9	22.0	20.4	21.0	17.9	25.7	23.4	25.9	20.3	25.7	24.4	22.9	22.2	21.0	24.0	20.8
2	19.1	24.1	23.5	23.8	23.3	22.0	21.9	24.5	21.4	24.5	24.3	24.9	22.5	23.3	26.2	22.2	19.0	25.0	23.3	21.7
3	28.9	20.9	23.6	23.3	22.0	20.2	18.2	22.2	20.6	24.0	21.9	24.9	24.1	23.1	20.6	26.6	21.2	25.9	20.9	21.9
4	19.6	23.5	20.6	18.8	24.0	21.8	23.6	22.0	23.4	18.1	25.7	24.6	24.2	24.7	22.0	23.3	23.1	22.8	21.3	21.1
5	22.3	20.9	24.5	27.5	18.3	22.8	19.5	24.5	27.7	19.2	26.1	17.8	23.6	24.3	22.7	25.3	25.4	23.3	20.1	20.8
6	20.6	18.8	19.9	23.4	26.2	21.9	22.2	27.6	26.3	23.7	27.8	24.4	21.7	23.7	21.1	21.5	23.8	22.9	22.2	23.3
7	26.0	24.9	24.7	24.9	24.4	21.0	25.8	30.9	23.5	29.0	23.4	27.3	24.1	23.8	22.5	21.6	23.1	25.8	26.3	25.6
8	19.9	28.5	29.6	27.8	21.4	25.1	27.3	27.5	23.9	24.3	27.1	25.8	26.7	24.0	23.5	28.4	27.8	29.8	22.7	23.6
9	22.7	26.0	23.8	29.4	22.7	21.7	26.5	28.0	24.8	23.7	25.0	24.0	26.2	29.5	27.0	22.8	25.4	21.9	26.1	25.7
10	34.6	29.4	26.9	30.4	24.1	26.2	30.9	30.7	28.5	27.8	25.9	31.1	23.9	28.7	28.0	29.6	26.3	28.8	29.6	25.8
11	28.0	33.3	28.0	26.5	28.5	26.7	29.6	27.1	27.6	29.1	33.0	26.4	30.4	29.4	32.3	22.5	26.7	28.8	26.1	25.6
12	27.4	26.8	26.6	27.1	21.7	25.0	25.7	24.2	27.5	28.8	24.5	27.6	23.2	28.6	23.2	26.6	25.1	28.3	26.0	25.9
13	31.1	26.8	27.5	32.9	23.1	33.3	25.4	29.1	28.5	29.2	26.9	28.8	30.4	22.1	24.1	33.4	29.0	25.8	27.2	24.6
14	26.0	25.9	26.5	24.8	26.6	24.4	31.0	24.0	31.7	27.0	23.0	26.5	29.4	29.9	28.0	29.0	31.1	23.2	26.2	23.0
15	24.4	28.2	28.2	29.8	27.2	22.7	30.5	28.9	25.2	27.0	32.4	28.2	29.3	26.2	26.5	27.1	25.0	28.5	26.7	27.7
16	25.2	23.6	26.3	25.6	28.6	28.5	27.7	23.6	21.1	26.9	25.1	30.6	32.0	25.0	28.7	29.8	27.2	29.7	30.7	26.8
17	27.6	26.5	20.9	25.7	27.0	26.1	25.2	30.0	28.5	28.7	25.2	26.6	29.0	29.9	27.1	23.9	27.0	22.2	25.4	27.1
18	28.0	26.5	24.2	26.0	23.8	29.0	29.8	27.0	23.6	24.1	22.7	26.2	27.2	27.6	24.7	24.9	21.8	27.4	24.0	22.3
19	27.1	25.7	26.9	22.6	25.1	25.0	21.2	23.4	22.6	25.4	22.6	27.0	26.3	23.3	24.0	25.2	26.3	24.7	24.5	22.9
20	23.1	24.6	26.1	24.7	18.5	24.4	23.0	23.0	20.6	25.4	22.3	21.7	22.4	22.6	23.6	23.7	22.7	22.7	23.4	24.3
21	27.3	24.8	22.8	25.7	20.8	19.8	20.2	21.1	22.3	22.2	18.1	23.6	20.3	20.9	24.2	25.9	28.0	23.8	29.8	23.7
22	23.4	22.3	22.9	23.3	19.9	26.2	19.8	23.0	25.5	22.7	24.0	25.5	26.1	26.8	21.3	21.8	26.3	23.9	23.4	24.0
23	25.6	23.7	21.5	23.2	23.1	27.8	24.2	24.7	24.9	22.6	23.6	23.8	21.1	23.9	24.7	23.1	25.8	24.9	22.7	23.2
24	22.8	25.3	25.0	23.1	24.7	27.3	25.3	24.8	20.6	22.8	24.0	23.3	19.6	21.8	25.8	18.4	26.1	20.2	24.5	23.5

It should be noted that the number of days for the studied horizon is 273.

Table 9
Numerical optimization results (objective function) without and with RTP.

#	Unit	Value	
		Without RTP	With RTP
Total expected cost	\$	130.394	81.733
Import cost	\$	866.490	823.477
Export revenue	\$	736.096	741.744
Total cost reduction	%	—	37.31

3. Numerical study

In this section, the optimal operation of the PV-based RC under the implementation of the EV is numerically studied without and with RTP. The studied RC is captured in Fig. 1. The proposed problem is modeled as an MILP and the GAMS software is employed to solve it (Soroudi, 2017).

3.1. Input data

Input data necessary for conducting simulations are presented below:

Critical and non-critical load profiles, real-time and upstream grid prices, sunlight irradiations and ambient temperature around the PV system, technical data of the PV system and technical parameters of the upstream grid are taken from (Numbi and Malinga, 2017). Furthermore, the technical data related to the EV and

$$p_{DRP,t,s}^{load,NC} = p_{t,s}^{load,NC} + E \times p_{t,s}^{load,NC} \times \frac{(\lambda_t^{imp} - RT_t^{price})}{RT_t^{price}} \quad (17)$$

where $p_{DRP,t,s}^{load,NC}$ is the non-critical load under RTP, E is the demand-price elasticity coefficient ($[-0.5, 0]$) and RT_t^{price} is the real-time power price.

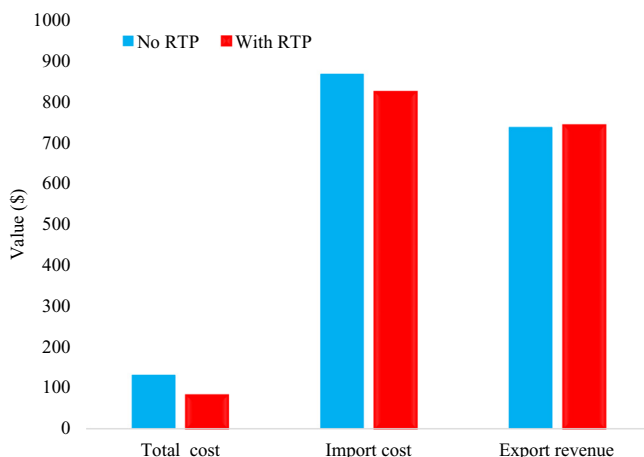


Fig. 2. Total cost of RC in detail without and with RTP.

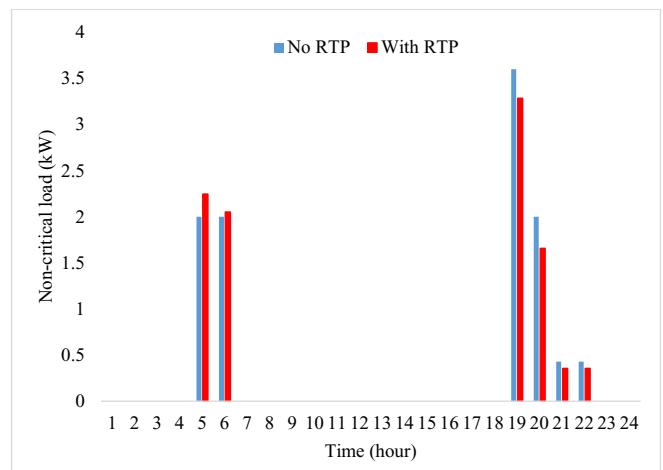


Fig. 3. Non-critical demand with RTP.

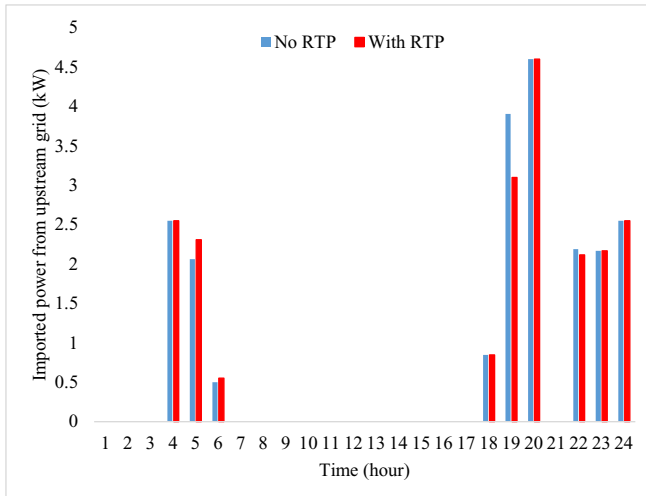


Fig. 4. Power imported from the upstream grid.

availability of the EV for charge and discharge processes are taken from previous studies (Jannati and Nazarpour, 2017).

The probability of each scenario and the value of uncertain parameters in each scenario are presented in Tables 1–8.

3.2. Results

In this section, simulations are carried out and the expected values of the result in different cases are presented. According to the obtained results, without taking RTP into account, the total expected operation cost of the RC in the defined horizon is \$130.394, including the \$866.490 cost of power imported from the

upstream grid and the \$736.096 revenue obtained from power exported to the upstream grid.

In order to motivate energy consumers to revise their energy consumption pattern, the RTP of the DRP is employed. Thus, with considering this type of pricing, the total expected operation cost of the RC in the defined horizon is \$81.733, including the \$823.477 cost of power imported from the upstream grid and the \$741.744 revenue obtained from power exported to the upstream grid. It is clear from the obtained results that by implementing the RTP of the DRP, the total expected cost of the RC is reduced up to 37.31%. In fact, by efficient charge and discharge processes of the EV system with RTP, economic goals of the RC are more satisfied, which appears to be suitable for the RC. For more comparison, numerical results without and with the RTP of the DRP are presented in Table 9. Also, total cost of RC including cost of purchasing power from upstream grid and revenue of selling power to the upstream grid is illustrated in Fig. 2.

Non-critical demand with the RTP of DRP is shown in Fig. 3. According to this figure, the energy consumption pattern with RTP changes in a way to reduce the total payments of the RC.

Total imported power from the upstream grid is shown in Fig. 4. Based on this figure, power imported from the upstream grid decreases with RTP; therefore, the total cost of the RC decreases.

Moreover, as shown in Fig. 5, total exported power from the RC to the upstream grid increases with RTP, which leads to more benefits.

Charge and discharge rates of the EV without and with RTP are depicted in Figs. 6 and 7, respectively. As shown in these figures, the EV is optimally charged and discharged with RTP to balance the intermittent output of the PV system and supply energy demand.

To illustrate the effect of the stochastic nature of the SOC at the arrival time of the EV, the total operation cost of RC without and with RTP is presented for all the scenarios in Table 10.

It is clear from Table 10 that under the SOC value in different

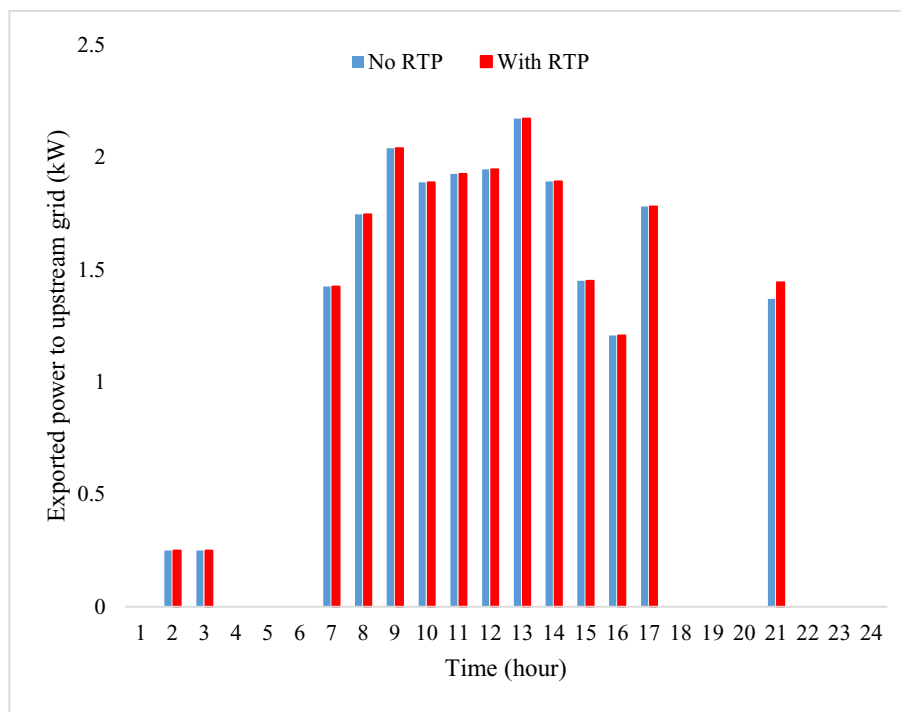


Fig. 5. Power exported to the upstream grid.

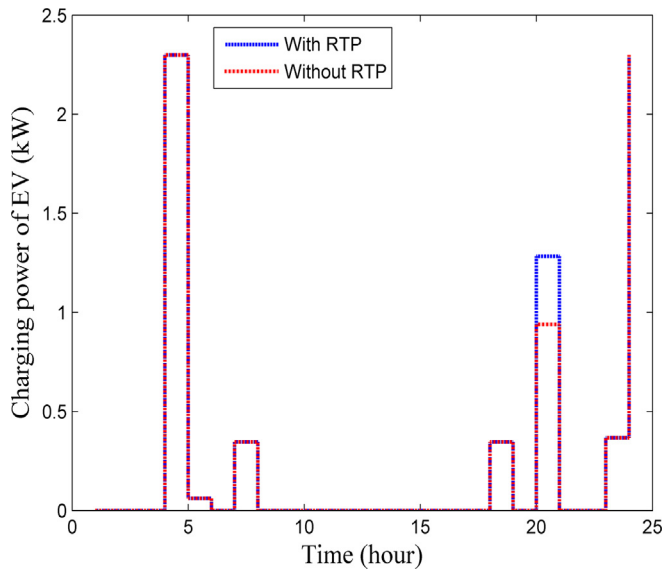


Fig. 6. The charge power of the EV.

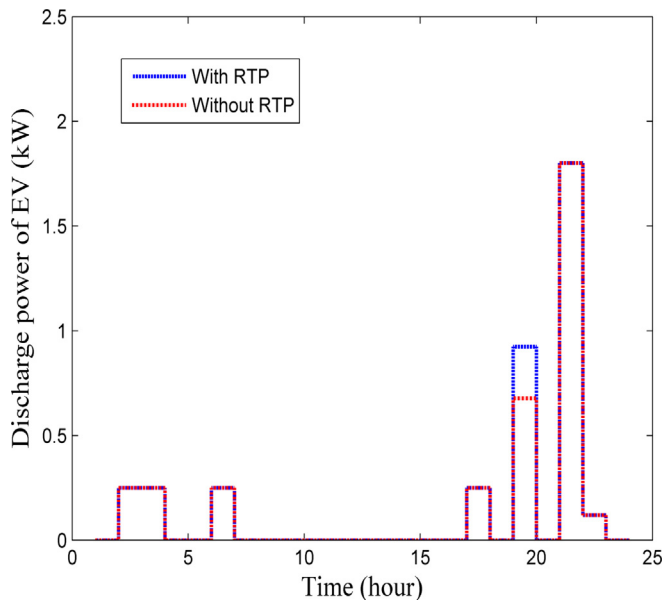


Fig. 7. The discharge power of the EV.

scenarios, the EV integrated into other energy units can present various kinds of performance, which can result in different economic performances.

4. Conclusion

Different types of DG units can be integrated in RCs to supply energy demands with their local generation. RCs including energy units such as EV and PV units that are accurately modeled can exchange energy with upstream grids to gain benefits. In this paper, a mathematical-based optimization framework was presented for the optimal integration of a PV unit and an EV into a grid-connected RC, in which the employed energy units were modeled through precise mathematical-based models to make simulation results as precise as possible. Moreover, the RTP mechanism of demand response was implemented to enhance the system economic performance and the consumer's behavior was analyzed toward the proposed prices within the mentioned mechanism. According to the simulation results, the proposed models for energy units in the RC were optimally configured and the optimal economic operation of the RC was obtained. Moreover, power generated by the PV unit was efficiently used to supply energy demand and charge the EV. Later, the stored energy was released to be either exported or used for supplying the demand. In addition, in accordance with power prices, within the periods with lower prices, the upstream grid power was imported to help the RC satisfy energy demands. It should be noted that different scenarios were generated to model stochastic driving patterns at the arrival time of the EV. It can be observed that the revenue obtained from exporting excess power generated by the PV unit can provide economic benefits for the RC. After applying RTP, the discussed economic results were enhanced since the total expected cost of the operating RC with RTP was reduced by 37.31%, which showed the optimal performance of energy units integrated into the RC with RTP. Energy units including PV systems and EVs can have more efficient performance with RTP, which could lead to a reduction in the total operation cost of the RC. It should be mentioned that the value of the obtained numerical results, such as cost-saving percentage, depends on the test system. The proposed mathematical model is easily applicable to other cases and can be extended to other systems with different energy mixes. Via extending the proposed model, one can study the probabilistic performance of the RC using different methodologies such as the chance-constraint method in future works.

Table 10
Total cost without and with RTP.

Without RTP				With RTP			
Scenario	Total cost (\$)	Scenario	Total cost (\$)	Scenario	Total cost (\$)	Scenario	Total cost (\$)
1	216.375	11	85.408	1	167.416	11	38.856
2	166.516	12	160.884	2	117.512	12	107.531
3	196.332	13	140.683	3	137.122	13	88.452
4	133.081	14	120.147	4	88.736	14	69.802
5	52.933	15	94.363	5	11.571	15	45.613
6	183.008	16	158.058	6	130.270	16	111.007
7	102.030	17	214.188	7	101.643	17	166.465
8	97.884	18	156.479	8	47.950	18	104.769
9	105.096	19	186.035	9	58.434	19	138.203
10	157.387	20	161.780	10	101.174	20	109.911

Declaration of competing interest

The authors declare that they have no known competing financial interests or personal relationships that could have appeared to influence the work reported in this paper.

References

- Abedini, M., Moradi, M.H., Hosseini, S.M., 2016. Optimal management of micro-grids including renewable energy sources using GPSO-GM algorithm. *Renew. Energy* 90, 430–439. <https://doi.org/10.1016/j.renene.2016.01.014>.
- Aghajani, G.R., Shayanfar, H.A., Shayeghi, H., 2017. Demand side management in a smart micro-grid in the presence of renewable generation and demand response. *Energy* 126, 622–637. <https://doi.org/10.1016/j.energy.2017.03.051>.
- Aghajani, G.R., Shayanfar, H.A., Shayeghi, H., 2015. Presenting a multi-objective generation scheduling model for pricing demand response rate in micro-grid energy management. *Energy Convers. Manag.* 106, 308–321. <https://doi.org/10.1016/j.enconman.2015.08.059>.
- Aliasghari, P., Mohammadi-Ivatloo, B., Alipour, M., Abapour, M., Zare, K., 2018. Optimal scheduling of plug-in electric vehicles and renewable micro-grid in energy and reserve markets considering demand response program. *J. Clean. Prod.* 186, 293–303. <https://doi.org/10.1016/j.jclepro.2018.03.058>.
- Aluisio, B., Conserva, A., Dicorato, M., Forte, G., Trovato, M., 2017. Optimal operation planning of V2G-equipped Microgrid in the presence of EV aggregator. *Electr. Power Syst. Res.* 152, 295–305. <https://doi.org/10.1016/j.epsr.2017.07.015>.
- Amrollahi, M.H., Bathaee, S.M.T., 2017. Techno-economic optimization of hybrid photovoltaic/wind generation together with energy storage system in a stand-alone micro-grid subjected to demand response. *Appl. Energy* 202, 66–77. <https://doi.org/10.1016/j.apenergy.2017.05.116>.
- Baccino, F., Grillo, S., Massucco, S., Silvestro, F., 2015. A two-stage margin-based algorithm for optimal plug-in electric vehicles scheduling. *IEEE Trans. Smart Grid* 1–5. <https://doi.org/10.1109/TSG.2014.2380826>.
- Bahramara, S., Golpira, H., 2018. Robust optimization of micro-grids operation problem in the presence of electric vehicles. *Sustain. Cities Soc.* 37, 388–395. <https://doi.org/10.1016/j.scs.2017.11.039>.
- Bukar, A.L., Tan, C.W., 2019. A review on stand-alone photovoltaic-wind energy system with fuel cell: system optimization and energy management strategy. *J. Clean. Prod.* 221, 73–88. <https://doi.org/10.1016/j.jclepro.2019.02.228>.
- Fathabadi, H., 2018a. Novel battery/photovoltaic hybrid power source for plug-in hybrid electric vehicles. *Sol. Energy* 159, 243–250. <https://doi.org/10.1016/j.solener.2017.10.071>.
- Fathabadi, H., 2018b. Utilizing solar and wind energy in plug-in hybrid electric vehicles. *Energy Convers. Manag.* 156, 317–328. <https://doi.org/10.1016/j.enconman.2017.11.015>.
- Fathabadi, H., 2017. Novel standalone hybrid solar/wind/fuel cell power generation system for remote areas. *Sol. Energy* 146, 30–43. <https://doi.org/10.1016/j.solener.2017.01.071>.
- Fathabadi, H., 2015. Utilization of electric vehicles and renewable energy sources used as distributed generators for improving characteristics of electric power distribution systems. *Energy* 90, 1100–1110. <https://doi.org/10.1016/j.energy.2015.06.063>.
- Forati, A., Soleimani, S., Karimpour, F., Malek, M.R., 2015. Including users' semantics in evaluating the credibility of crowdsourced landscape descriptions. In: Olteanu-Raimon, A.M. (Ed.), *International Archives of the Photogrammetry, Remote Sensing and Spatial Information Sciences - ISPRS Archives. The International Archives of the Photogrammetry, Remote Sensing and Spatial Information Sciences*, pp. 1–4.
- Galindo Noguera, A.L., Mendoza Castellanos, L.S., Silva Lora, E.E., Melian Cobas, V.R., 2018. Optimum design of a hybrid diesel-ORC/photovoltaic system using PSO: case study for the city of Cujubim, Brazil. *Energy* 142, 33–45. <https://doi.org/10.1016/j.energy.2017.10.012>.
- Gholami, S., Saha, S., Aldeen, M., 2018. Robust multiobjective control method for power sharing among distributed energy resources in islanded microgrids with unbalanced and nonlinear loads. *Int. J. Electr. Power Energy Syst.* <https://doi.org/10.1016/j.ijepes.2017.07.012>.
- He, Y., Kockelman, K.M., Perrine, K.A., 2019. Optimal locations of U.S. fast charging stations for long-distance trip completion by battery electric vehicles. *J. Clean. Prod.* 214, 452–461. <https://doi.org/10.1016/j.jclepro.2018.12.188>.
- He, Y., Venkatesh, B., Guan, L., 2012. Optimal scheduling for charging and discharging of electric vehicles. *IEEE Trans. Smart Grid* 3 (3), 1095–1105. <https://doi.org/10.1109/TSG.2011.2173507>.
- Hong, Y.Y., Chang, W.C., Chang, Y.R., Lee, Y.D., Ouyang, D.C., 2017. Optimal sizing of renewable energy generations in a community microgrid using Markov model. *Energy* 135, 68–74. <https://doi.org/10.1016/j.energy.2017.06.098>.
- Jalali, M., Zare, K., Seyedi, H., 2017. Strategic decision-making of distribution network operator with multi-microgrids considering demand response program. *Energy* 141, 1059–1071. <https://doi.org/10.1016/j.energy.2017.09.145>.
- Jannati, J., Nazarpour, D., 2017. Optimal energy management of the smart parking lot under demand response program in the presence of the electrolyser and fuel cell as hydrogen storage system. *Energy Convers. Manag.* 138, 659–669. <https://doi.org/10.1016/j.enconman.2017.02.030>.
- Jung, J., Villaran, M., 2017. Optimal planning and design of hybrid renewable energy systems for microgrids. *Renew. Sustain. Energy Rev.* 75, 180–191. <https://doi.org/10.1016/j.rser.2016.10.061>.
- Kamankesh, H., Agelidis, V.G., Kavousi-Fard, A., 2016. Optimal scheduling of renewable micro-grids considering plug-in hybrid electric vehicle charging demand. *Energy* 100, 285–297. <https://doi.org/10.1016/j.energy.2016.01.063>.
- Kerdphol, T., Rahman, F.S., Mitani, Y., Watanabe, M., Kufeoglu, S., 2018. Robust Virtual Inertia Control of an Islanded Microgrid Considering High Penetration of Renewable Energy. *IEEE Access* 6, 625–636.
- Li, Y., Yang, Z., Li, G., Mu, Y., Zhao, D., Chen, C., Shen, B., 2018. Optimal scheduling of isolated microgrid with an electric vehicle battery swapping station in multi-stakeholder scenarios: a bi-level programming approach via real-time pricing. *Appl. Energy* 232, 54–68. <https://doi.org/10.1016/j.apenergy.2018.09.211>.
- Liu, Z., Chen, Y., Zhuo, R., Jia, H., 2018. Energy storage capacity optimization for autonomy microgrid considering CHP and EV scheduling. *Appl. Energy* 210, 1113–1125. <https://doi.org/10.1016/j.apenergy.2017.07.002>.
- Liu, Z., Wu, Q., Oren, S.S., Huang, S., Li, R., Cheng, L., 2018. Distribution locational marginal pricing for optimal electric vehicle charging through chance constrained mixed-integer programming. *IEEE Trans. Smart Grid* 9 (2), 644–654. <https://doi.org/10.1109/TSG.2016.2559579>.
- Lu, X., Zhou, K., Yang, S., Liu, H., 2018. Multi-objective optimal load dispatch of microgrid with stochastic access of electric vehicles. *J. Clean. Prod.* 195, 187–199. <https://doi.org/10.1016/j.jclepro.2018.05.190>.
- Machura, P., Li, Q., 2019. A critical review on wireless charging for electric vehicles. *Renew. Sustain. Energy Rev.* 104, 209–234. <https://doi.org/10.1016/j.rser.2019.01.027>.
- Majidi, M., Nojavan, S., Nourani Efsatanaj, N., Najafi-Ghalelou, A., Zare, K., 2017. A multi-objective model for optimal operation of a battery/PV/fuel cell/grid hybrid energy system using weighted sum technique and fuzzy satisfying approach considering responsible load management. *Sol. Energy* 144, 79–89. <https://doi.org/10.1016/j.solener.2017.01.009>.
- Mirzaei, M.A., Yazdankhah, A.S., Mohammadi-Ivatloo, B., Marzband, M., Shafiekhah, M., Catalão, J.P.S., 2019. Stochastic network-constrained co-optimization of energy and reserve products in renewable energy integrated power and gas networks with energy storage system. *J. Clean. Prod.* 223, 747–758. <https://doi.org/10.1016/j.jclepro.2019.03.021>.
- Mortaz, E., Vinel, A., Dvorkin, Y., 2019. An optimization model for siting and sizing of vehicle-to-grid facilities in a microgrid. *Appl. Energy* 242, 1649–1660. <https://doi.org/10.1016/j.apenergy.2019.03.131>.
- Nemati, M., Braun, M., Tenbohlen, S., 2018. Optimization of unit commitment and economic dispatch in microgrids based on genetic algorithm and mixed integer linear programming. *Appl. Energy* 210, 944–963. <https://doi.org/10.1016/j.apenergy.2017.07.007>.
- Nikmehr, N., Najafi-Ravadanegh, S., Khodaei, A., 2017. Probabilistic optimal scheduling of networked microgrids considering time-based demand response programs under uncertainty. *Appl. Energy* 198, 267–279. <https://doi.org/10.1016/j.apenergy.2017.04.071>.
- Numbi, B.P., Malinga, S.J., 2017. Optimal energy cost and economic analysis of a residential grid-interactive solar PV system- case of eThekweni municipality in South Africa. *Appl. Energy* 186, 28–45. <https://doi.org/10.1016/j.apenergy.2016.10.048>.
- Odetayo, B., Kazemi, M., MacCormack, J., Rosehart, W.D., Zareipour, H., Seifi, A.R., 2018. A chance constrained programming approach to the integrated planning of electric power generation, natural gas network and storage. *IEEE Trans. Power Syst.* 33 (6), 6883–6893. <https://doi.org/10.1109/TPWRS.2018.2833465>.
- Pascual, J., Barricarte, J., Sanchis, P., Marroyo, L., 2015. Energy management strategy for a renewable-based residential microgrid with generation and demand forecasting. *Appl. Energy* 158, 12–25. <https://doi.org/10.1016/j.apenergy.2015.08.040>.
- Pearre, N.S., Swan, L.G., 2016. Electric vehicle charging to support renewable energy integration in a capacity constrained electricity grid. *Energy Convers. Manag.* 109, 130–139. <https://doi.org/10.1016/j.enconman.2015.11.066>.
- Pesaran, M., H.A., Huy, P.D., Ramachandramurthy, V.K., 2017. A review of the optimal allocation of distributed generation: objectives, constraints, methods, and algorithms. *Renew. Sustain. Energy Rev.* 75, 293–312. <https://doi.org/10.1016/j.rser.2016.10.071>.
- Rodrigues, Y.R., Zambroni de Souza, A.C., Ribeiro, P.F., 2018. An inclusive methodology for Plug-in electrical vehicle operation with G2V and V2G in smart microgrid environments. *Int. J. Electr. Power Energy Syst.* 102, 312–323. <https://doi.org/10.1016/j.ijepes.2018.04.037>.
- Rokni, S.G.M., Radmehr, M., Zakariazadeh, A., 2018. Optimum energy resource scheduling in a microgrid using a distributed algorithm framework. *Sustain. Cities Soc.* 37, 222–231. <https://doi.org/10.1016/j.scs.2017.11.016>.
- Salehi, J., Gazijahani, F.S., 2018. Decentralized trading of plug-in electric vehicle aggregation agents for optimal energy management of smart renewable penetrated microgrids with the aim of CO₂ emission reduction. *J. Clean. Prod.* 200, 622–640. <https://doi.org/10.1016/j.jclepro.2018.07.315>.
- Sedighzadeh, M., Esmaili, M., Mohammadkhani, N., 2018. Stochastic multi-objective energy management in residential microgrids with combined cooling, heating, and power units considering battery energy storage systems and plug-in hybrid electric vehicles. *J. Clean. Prod.* 195, 301–317. <https://doi.org/10.1016/j.jclepro.2018.05.103>.
- Shezan, S.A., Julai, S., Kibria, M.A., Ullah, K.R., Saidur, R., Chong, W.T., Akikur, R.K., 2016. Performance analysis of an off-grid wind-PV (photovoltaic)-diesel-battery hybrid energy system feasible for remote areas. *J. Clean. Prod.* 125, 121–132. <https://doi.org/10.1016/j.jclepro.2016.03.014>.

- SoltaniNejad Farsangi, A., Hedayeghpars, S., Mehdinejad, M., Shayanfar, H., 2018. A novel stochastic energy management of a microgrid with various types of distributed energy resources in presence of demand response programs. *Energy* 160, 257–274. <https://doi.org/10.1016/j.energy.2018.06.136>.
- Soroudi, A., 2017. *Power System Optimization Modeling in GAMS, Power System Optimization Modeling in GAMS*. Springer.
- Sortomme, E., El-Sharkawi, M.A., 2012. Optimal scheduling of vehicle-to-grid energy and ancillary services. *IEEE Trans. Smart Grid* 3 (1), 351–359. <https://doi.org/10.1109/TSG.2011.2164099>.
- Sreedharan, Priya, Farbes, Jamil, Cutter, Eric, Woo, Chi-Keung, Wang, Jianhui, 2016. *Microgrid and renewable generation integration: University of California, San Diego*. *Appl. Energy* 169, 709–720.
- Tabar, V.S., Jirdehi, M.A., Hemmati, R., 2017. Energy management in microgrid based on the multi objective stochastic programming incorporating portable renewable energy resource as demand response option. *Energy* 118, 827–839. <https://doi.org/10.1016/j.energy.2016.10.113>.
- Tabatabaee, S., Mortazavi, S.S., Niknam, T., 2017. Stochastic scheduling of local distribution systems considering high penetration of plug-in electric vehicles and renewable energy sources. *Energy* 121, 480–490. <https://doi.org/10.1016/j.energy.2016.12.115>.
- Wu, C., Mohammadi, A., Mehrtash, M., Kargarian, A., 2019. Non-parametric joint chance constraints for economic dispatch problem with solar generation. In: 2019 IEEE Texas Power and Energy Conference. TPEC 2019. IEEE, pp. 1–6. <https://doi.org/10.1109/TPEC.2019.8662145>.
- Zehir, M.A., Batman, A., Sonmez, M.A., Font, A., Tsiamitros, D., Stimoniaris, D., Kollatou, T., Bagriyanik, M., Ozdemir, A., Dialynas, E., 2017. Impacts of microgrids with renewables on secondary distribution networks. *Appl. Energy* 201, 308–319. <https://doi.org/10.1016/j.apenergy.2016.12.138>.